

Article

Enhanced Recovery of Alginate-like Extracellular Polymers (ALE) from Waste-Activated Sludge Using Sodium Percarbonate: Performance and Characteristics

Xiaoping Liu ^{1,2,*}, Wanying Ren ^{1,2}, Yunbo Zhai ^{1,2,*}, Yu Xie ^{1,2}, Fashen Liang ^{1,2} and Zhixiang Xu ³

¹ College of Environmental Science and Engineering, Hunan University, Changsha 410082, China

² Key Laboratory of Environmental Biology and Pollution Control, Hunan University, Ministry of Education, Changsha 410082, China

³ School of Energy and Power Engineering, Jiangsu University, Zhenjiang 212013, China

* Correspondence: xiaopingliu@hnu.edu.cn (X.L.); ybzhai@hnu.edu.cn (Y.Z.)

Abstract: Resource recovery from waste-activated sludge is of great practical significance to achieve sustainable wastewater treatment. Alginate-like extracellular polymers (ALE), a typical class of extracellular polymer substances, are valuable bio-based products with broad application prospects. However, due to the low extraction efficiency of the current method, its practical applications are severely limited. In this study, sodium percarbonate (SPC) was first applied to enhance ALE extraction from conventional activated sludge to replace the sodium carbonate (SC) in the heating-SC method. The results showed that the ALE extracted by the heating-SPC method increased by 30.11% compared to the heating-SC method, and the alginate equivalent was slightly improved. Monosaccharide composition analysis showed that the ALE primarily comprised galactose and glucose, indicating the potential for biomedical applications. The particle size distribution and extracellular polymeric substances (EPS) composition of the sludge indicated that SPC could improve the cracking of the sludge flocs and the organic release. In addition, due to SPC's ability to oxidize, the molecular composition of the ALE extract changed. In conclusion, SPC used as a substitute for SC in the heating-SC method could be effectively employed to recover ALE from waste-activated sludge. In future studies, further optimization of the operational conditions needs to be considered.

Keywords: waste-activated sludge; biopolymer recovery; valorization; extraction; sodium percarbonate; alginate-like extracellular polymers



Citation: Liu, X.; Ren, W.; Zhai, Y.; Xie, Y.; Liang, F.; Xu, Z. Enhanced Recovery of Alginate-like Extracellular Polymers (ALE) from Waste-Activated Sludge Using Sodium Percarbonate: Performance and Characteristics. *Sustainability* **2023**, *15*, 14573. <https://doi.org/10.3390/su151914573>

Academic Editors: Elli Maria Barampouti and Sofia Th. Mai

Received: 13 September 2023

Revised: 28 September 2023

Accepted: 7 October 2023

Published: 8 October 2023



Copyright: © 2023 by the authors. Licensee MDPI, Basel, Switzerland. This article is an open access article distributed under the terms and conditions of the Creative Commons Attribution (CC BY) license (<https://creativecommons.org/licenses/by/4.0/>).

1. Introduction

Over the last few decades, the global production of waste-activated sludge (WAS) has been continuously increasing, which poses a potential threat to the environment [1]. According to the statistics, China produces 60 million tons of sewage sludge (80% water content) with an annually increasing rate of 10%, while the European Union produces approximately 50 million tons of sewage sludge per year and the United States produces 40 million tons [2]. With growing global urbanization and increasingly stringent regulations on sludge reuse or disposal, it prompts us to reevaluate the current sludge management strategies. The traditional disposal methods mainly include incineration, landfills, ocean disposal, or agricultural reuse, which are not sustainable ways to improve and clean the environment. WAS consists of a complex multi-component mixture of microorganisms, organic matter, inorganic materials, and moisture. As the resource crisis intensifies, the recycling of valuable resources from sludge has important practical significance. The recovery of bio-based products from sludge can offset part of the cost of sludge treatment and disposal, which is also conducive to a sustainable and circular economy.

Extracellular polymeric substances (EPS) are known to critically affect the properties and performance of activated sludge [3] and are also reported to be the most important

factor affecting sludge dewatering performance [4]. EPS are mainly composed of a wide variety of biopolymers with a high molecular weight (including proteins, lipids, and polysaccharides), which comprise 60–80% of the sludge volume [5]; therefore, recovering biopolymers from sludge has become a current research hotspot and attracts considerable attention in various applications [6,7]. As a complex of natural biopolymers, EPS can not only maintain the stability of sludge structure but also protect cells from external environmental stress (including toxic substances and heavy metals) [8]. The biomacromolecules in the EPS matrix have unique properties, which are potentially high value-added and versatile bio-based materials [9]. Among these complex biopolymers in the EPS matrix, exopolysaccharides have attracted increasing attention due to their special properties and functions. Extraction and recovery of alginate-like extracellular polymers (ALE) from aerobic granular sludge (AGS) have attracted a lot of attention [10,11]. These so-called ALE are substances analogous to alginate that are extracted from the AGS extracellular matrix, which are also identified by their ability to form gels with calcium ions and uronic acid residues. Similar to commercial alginate, ALE can be used in many different fields, such as food, medical, textile, environmental remediation, and other fields. For instance, ALE extracted from AGS can be used as flame-retardant surface-coating materials in aerospace and other fields [7,12]. In addition to the laboratory research, the extraction of ALE from AGS was scaled up in the Netherlands; these products are named Kaumera® [13]. Numerous studies have shown that the relative quantity of EPS in conventional activated sludge (CAS) was lower than that of AGS. A recent study demonstrated that the ALE derived from CAS ranged from 90 to 190 mg/g VSS, which is lower than AGS with 200–350 mg/g VSS [14]. However, the total amount of CAS is huge, and the absolute content of ALE in CAS is of great value. Accordingly, there is a significant need for ALE recovery from waste-activated sludge.

Currently, the ALE recovered from CAS is limited mainly due to the intrinsic low content and also the low efficiency with existing extraction methods. In addition, the other disadvantage of previous methods is that the economic value of extracted ALE is low [14]. Innovatively, Lin et al. [11,15] proposed an efficient heating- Na_2CO_3 method for ALE extraction from AGS, which was inspired by the extraction strategy of alginate from seaweed. Thereafter, this method was widely used for ALE or EPS extraction from sludge. Feng et al. systematically compared and evaluated seven commonly used protocols for EPS extraction from anammox granules and obtained the highest EPS yield by heating- Na_2CO_3 method [16]. Specifically, the heating- Na_2CO_3 method yielded 210 ± 5 mg/g VSS, while the Formamide- NaOH treatment generated 182 ± 25 mg/g VSS, and the other methods yielded EPS from 16 ± 2 to 92 ± 14 mg/g VSS. As for CAS, a few strategies were proposed to improve the extraction efficiency of ALE. It was reported that the addition of surfactants based on the heating- Na_2CO_3 method improved the ALE extraction efficiency by 79.5–127.2% [14]. Sodium percarbonate (SPC, $\text{Na}_2\text{CO}_3 \cdot 1.5\text{H}_2\text{O}_2$), also known as solid hydrogen peroxide, is an effective, harmless, and economical oxidant. SPC can be decomposed into hydrogen peroxide and sodium carbonate in aqueous media without any by-product formation. It has recently been used as a conditioner to enhance sludge dewaterability [17–19], anaerobic fermentation [20–22], or anaerobic digestion performance [23,24]. Many prior efforts were made to active SPC via homogeneous or heterogeneous catalysis, including ferrous iron [17,25], zero-valent iron [26], iron-containing minerals [19], sludge-derived biochar [18], ultrasound [20,23], and ultraviolet [27]. The above comprehensive studies showed that SPC-based pretreatments accelerated sludge solubilization through disintegrating the extracellular polymeric substances and the cell walls of the sludge. Taking into account the similarities of EPS destruction during the ALE extraction process, we therefore speculated that ALE extraction efficiency can be further improved by replacing sodium carbonate (Na_2CO_3 , SC) with SPC. On the one hand, the alkalinity of SPC and its ability to oxidize can disrupt EPS and release the biopolymers. From another point of view, Na_2CO_3 from SPC decomposition can be subsequently used to extract ALE. Furthermore, to the best of our knowledge, the proposed method has never been reported before in the

literature. Owing to this, it may greatly increase the production of ALE from WAS, which would provide huge economic value. This “waste to treasure” strategy not only benefits the circular economy and low-carbon economy but also helps to reduce the negative impact on the ecological environment.

In this work, a heating-SPC method for ALE extraction from waste-activated sludge was first proposed. The traditional heating-SC method was also conducted as a comparison. The main objectives of this study are: (i) to evaluate the efficiency of ALE extraction and alginate equivalent; (ii) to reveal the mechanisms through characterizing the physical and chemical properties of sludge; and (iii) to compare the properties of ALE products.

2. Materials and Methods

2.1. Waste-Activated Sludge and Reagents

The sludge samples were collected from the secondary settling tank of a municipal wastewater treatment plant in Changsha, China. The sludge samples were transferred to the laboratory as soon as possible and immediately stored at 4 °C. Before the experiment started, the supernatant was removed to further thicken the sludge. The basic physical and chemical properties of the sludge are shown in Table 1. In order to eliminate environmental interference, all experiments were conducted in 5 days.

Table 1. Basic properties of WAS.

Parameter	Value
Water content	98.16 ± 0.14%
Total suspended solid (TSS)	18.04 ± 0.36 g/L
Volatile suspended solid (VSS)	8.93 ± 0.10 g/L
pH	7.04 ± 0.03
Capillary suction time (CST)	37.9 ± 1.0 s
Medium diameter	33.22 ± 3.26 µm

SPC was purchased from Shanghai Macklin Biochemical Co., Ltd., Shanghai, China. Hydrochloric acid (HCl) and Sodium hydroxide (NaOH) were obtained from Sinopharm Chemical Reagent Co., Ltd., Shanghai, China.

2.2. Extraction Procedures

The ALEs were extracted based on the method of heating-SC, which was widely used in previous studies [28,29]. As shown in Figure 1, the whole process includes several parts, namely, sludge pretreatment, solid–liquid separation, purification/concentration, and freeze-drying. Briefly, 50 mL of sludge with 0.50% (*w/v*) SC in a centrifuge tube heated in an 80 °C water bath (SHZ-88, Changzhou Jintan Kexing Instrument Factory, Changzhou, China) for 35 min. Afterward, the heated sludge was centrifuged at 4000 × *g* for 20 min (TG16KR, Changsha Dongwang Experimental Instrument Co., Ltd., Changsha, China), and the collected supernatants were adjusted to pH 2.2 with 1 M HCl. Subsequently, the acquired supernatants were centrifuged at 4000 × *g* for 20 min again. The obtained granules were re-dissolved in 1 M NaOH (pH 8.5) and dialyzed in a 3500 Da dialysis bag for 24 h to remove the impurities. Ultimately, the aqueous ALE products were freeze-dried at −50 °C (SJIA-10N-50C, Ningbo Shuangjia Instrument Co., Ltd., Ningbo, China). The ALE extracted by the heating-SC method was recorded as “SC”. As for the heating-SPC method, all the steps were the same as above, except the 0.5% (*w/v*) SC was replaced with 0.74% (*w/v*) SPC, which ensured the concentrations of Na₂CO₃ were the same in these two protocols. Accordingly, the ALE extracted by the heating-SPC method was recorded as “SPC”. Three parallel experiments were conducted for both of the extracting methods.

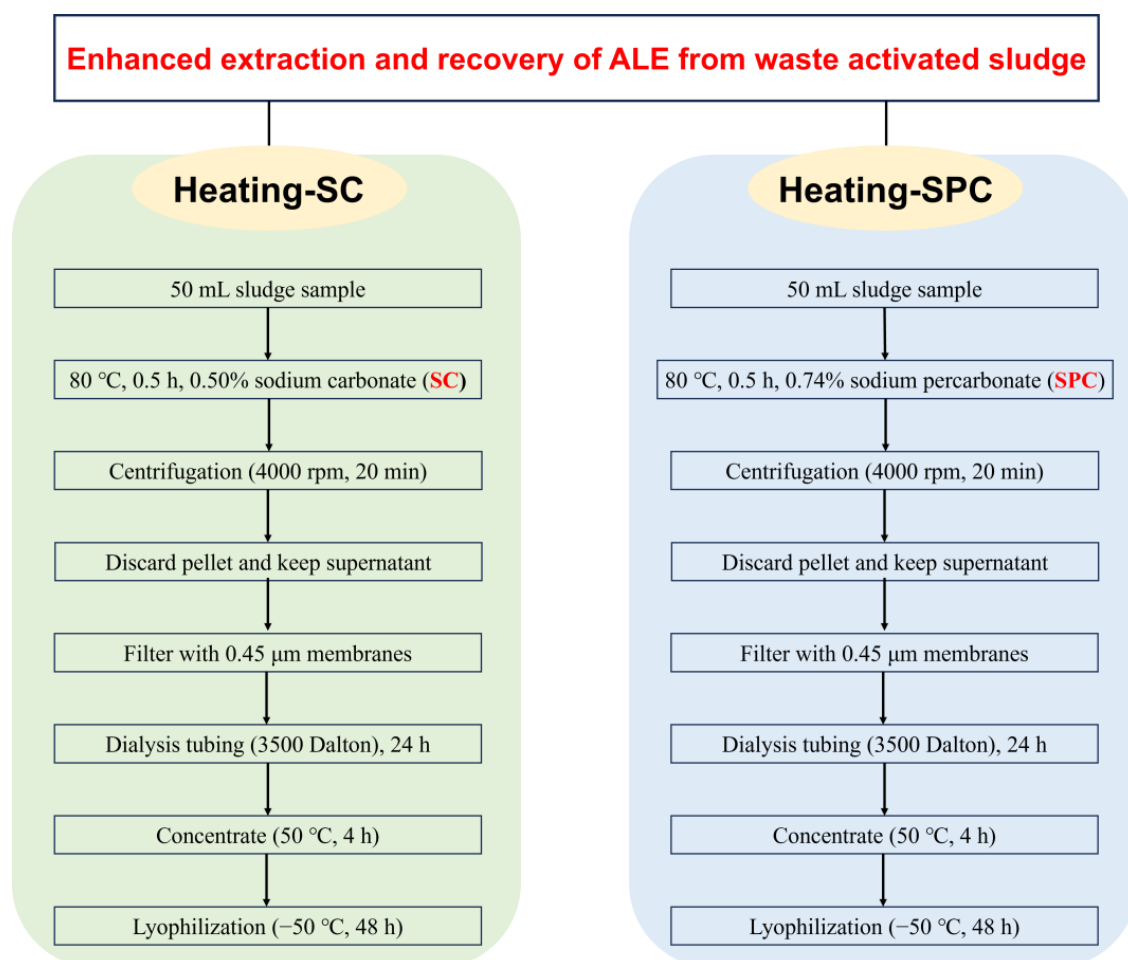


Figure 1. Experimental scheme for ALE extraction and recovery.

2.3. Analytical Methods

The water content, TSS, VSS, and pH, were detected according to the standard methods [30]. CST of the raw sludge samples was analyzed using a CST device (304 M, Triton, Yeovil, UK) according to the manufacturer's instructions.

To assess the effect of sludge pretreatment on sludge characteristics, the particle size distribution of sludge flocs after heat treatment with SC or SPC was analyzed using a particle size analyzer (Mastersizer 2000, Malvern, UK) [31]. As a comparison, the sludge without any other additives was also evaluated after heat treatment (recorded as "RS").

The EPS of pretreated sludge (RS/SC/SPC) was further extracted using a modified thermal extraction method, which could be divided into three layers, tightly bound EPS (TB-EPS), loosely bound EPS, and soluble EPS (S-EPS). Briefly, the sludge samples after different pretreatments were first centrifuged to obtain the supernatant (TG16KR, Changsha Dongwang Experimental Instrument Co., Ltd., Changsha, China), which is defined as S-EPS. After being centrifuged, the pellets were re-suspended with 0.05% (*w/w*) NaCl solution (70 °C preheat) equivalent to original supernatant volume and mixed with a vortex shaker (VM-370, IntlLab Vortex Mixer, Grove, OR, USA) for 1 min. The suspension was centrifuged to collect the supernatant again, which was regarded as LB-EPS. The pellets were re-suspended and mixed the same as the previous step, the suspension was heated in a water bath at 60 °C for 30 min and finally centrifuged to acquire the supernatant as TB-EPS.

To reveal the organic composition in different EPS fractions, three-dimensional fluorescence excitation-emission matrix (3d-EEM) spectroscopy (F-4600, Hitachi, Tokyo, Japan) was used [32]. The instrument settings were as follows: excitation wavelength ranged from 200 to 450 nm, emission wavelength ranged from 250 to 550 nm, step size, and slit width was 5 nm, scan speed was 1200 nm/min. To reduce the distractions of Rayleigh scattering, the fluorometer's response to a blank solution (ultra-pure water) was subtracted from the fluorescence spectra recorded for samples. The fluorescence regional integration (FRI) analysis of EEM spectra was conducted according to the method reported in the literature [33].

The concentrations of polysaccharide (PS) were measured using the phenol-sulfuric acid method using glucose as a standard, and the proteins were analyzed by the modified Lowry method with bovine serum albumin used as the standard. The purity of extracted ALEs was determined by the phenol-sulfuric acid assay and the commercial alginate (analytical reagent) was used as the standard at varying concentrations to create a standard curve [14]. The surface functional groups of ALE were identified by a Thermo Scientific K-Alpha + XPS system (ThermoFisher Scientific Inc., Waltham, MA, USA).

The ALEs were dissolved into deionized water at the concentration of 500 mg/L, and the commercial sodium alginate was also used as a reference. Ultraviolet-visible (UV-Vis) absorption of ALEs or alginate was obtained by UV-vis spectroscopy (UV1810S, Yoke Instrument, Shanghai, China). Furthermore, a dimensionless parameter of UV-vis absorption spectra (S_R) was calculated according to the properties of spectra, which is defined as the ratio of spectra slope (275–295 nm) to slope (350–400 nm). S_R is reported to reflect the molecular weight of dissolved organic matter [34].

The ^1H nuclear magnetic resonance (NMR) spectra of the ALEs were recorded by 600 MHz Avance spectrometer (Bruker BioSpin, Rheinstetten, Germany), equipped with 5 mm NMR tubes at 25 °C in D_2O .

2.4. Statistical Analysis

Data were analyzed using Microsoft Excel version 2021. The Origin 2023b software (Learning edition) was used to draw graphs.

3. Results and Discussion

3.1. The Amount and Quality of ALE

The amount and purity of the ALEs extracted from waste-activated sludge using the heating-SC and heating-SPC methods are shown in Figure 2. It shows that the ALE increased significantly from 113.48 ± 4.99 mg/g VSS to 164.84 ± 2.93 mg/g VSS when using the heating-SPC method, compared with the conventional heating-SC method. A previous study also found that the ALEs extracted from CAS varied from 90 to 190 mg/g VSS [29], which was consistent with our current study. In addition, the alginate equivalent of ALE was also intensified from $63.20 \pm 3.02\%$ to $65.34 \pm 1.00\%$ accordingly. But the improvement was insignificant. The alginate equivalents of ALE to the commercial alginate in this study were higher than the values reported in the literature (42–52%) [29], which may be related to the nature of the sludge. Feng et al. compared seven methods to extract EPS from anammox granules and obtained the highest EPS yield using the heating-SC method [16]. Although the current extraction protocol of heating-SC was proven to be effective in AGS, it was not effective in conventional waste-activated sludge [14]. In this work, heating-SPC was proven to be an effective alternative. Even better performance can doubtlessly be obtained with further optimization (processing temperature, reaction time). H_2O_2 in SPC is the only difference with SC, which is better for the environment. Moreover, the SPC-based pretreatment also contributes to coliform inactivation and phytotoxicity reduction [25], which can broaden its application for detoxification.

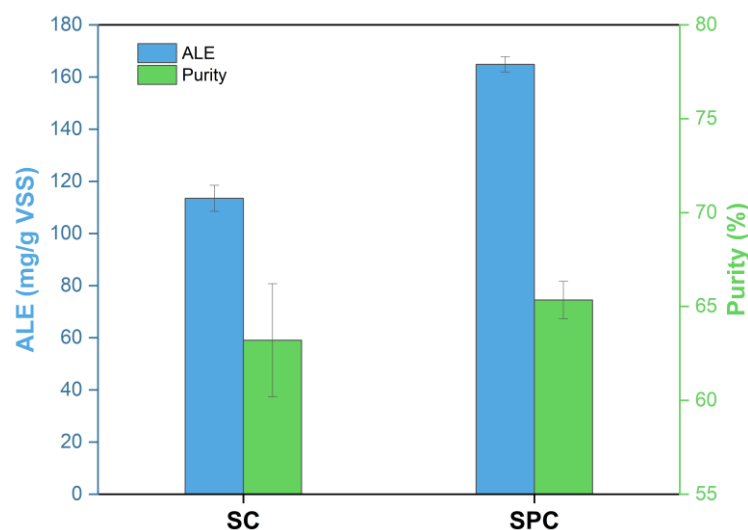


Figure 2. The amount and quantity of alginate-like extracellular polymers (ALE) extracted from waste-activated sludge using SC- and SPC-based methods.

3.2. The Variation of Sludge Flocs

3.2.1. The Particle Size Distribution of Sludge Flocs

To determine the effects of extracting protocols on sludge particles, the particle size distribution (PSD) is applied to evaluate the microstructure of sludge treated using the heating-SC and heating-SPC methods. As indicated in Figure 3, the particle size of the sludge decreased after being treated with SC or SPC. The floc sizes (D10, D50, and D90) of sludge in the SC and SPC groups were smaller compared with the RS group. For instance, the D90 of sludge decreased from $90.60 \pm 11.83 \mu\text{m}$ (RS) to $82.40 \pm 4.73 \mu\text{m}$ (SC) and $71.46 \pm 6.24 \mu\text{m}$ (SPC), respectively. It was reported that alkaline treatment could decompose sludge flocs and thus enhance the release of organics [35]. Here in this study, it can be found that the particle size of SPC-treated sludge was obviously smaller than that of the SC-treated sludge, suggesting a greater cracking of sludge flocs. This can partially explain the enhanced extraction of ALE from sludge using SPC.

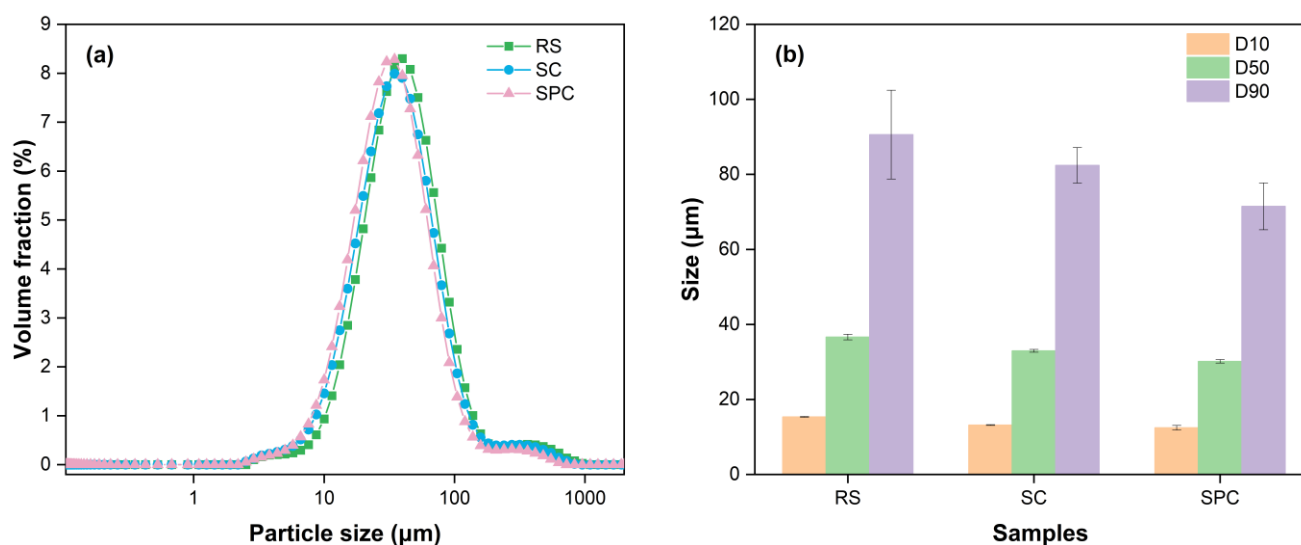


Figure 3. The particle size distribution of sludge. (a) Particle size distribution curves; (b) percentiles describing the particle size distribution. (RS: raw sludge without any treatments, SC: sludge pretreated by heating-sodium carbonate, SPC: sludge pretreated by heating-sodium percarbonate).

3.2.2. Composition of Sludge EPS

The sensitive 3d-EEM spectroscopy was used to define the fluorescent substances in the different EPS layers and investigate fluorescence differences between the two extracting methods. Fluorescence characteristics largely depend on the structural and functional properties of the dissolved molecular substances. It is widely reported that the EEM spectra can be divided into five regions: tyrosine-like protein (Region I), tryptophan-like protein (Region II), fulvic acid-like (Region III), microbial by-product-like organics (Region IV), and humic acid-like organics (Region V) [36]. Generally, the fluorescence intensity of the EEM spectrum can reflect the concentration of specific dissolved organics, and the shift of the fluorescence peak is mainly due to the variation of specific functional groups. As shown in Figure 4, the location and fluorescence intensity of the peaks changed greatly. As for RS, the main fluorescence peaks are located at Regions I, II, and IV. The fluorescence intensities of the aromatic protein and soluble microbial by-products in S-EPS and LB-EPS were higher than those of TB-EPS. This was in accordance with the previous study, which found that a thermal treatment caused the destruction of sludge and thus fluorescence organics released from TB-EPS to LB-EPS and S-EPS [37]. While in the S-EPS of SC, the protein-like substances (Regions I and II) significantly decreased and a prominent peak A (Em/Ex: 280 nm/350 nm) remained. Peak A was in line with the result reported by Feng et al. [16], who confirmed the superior performance of EPS extraction using the heating-SC method over the other six methods. Compared to both RS and SC, most of the fluorescence intensities in the different regions were considerably reduced. This may be due to the decomposition of the fluorescent components by the radicals. It was reported that hydrogen peroxide can be thermally activated to destruct sludge [38] or treat landfill leachate [39]. Similarly, the hydrogen peroxide induced from dissolved SPC can also be activated using a thermal treatment, which is able to oxidize the organics in EPS.

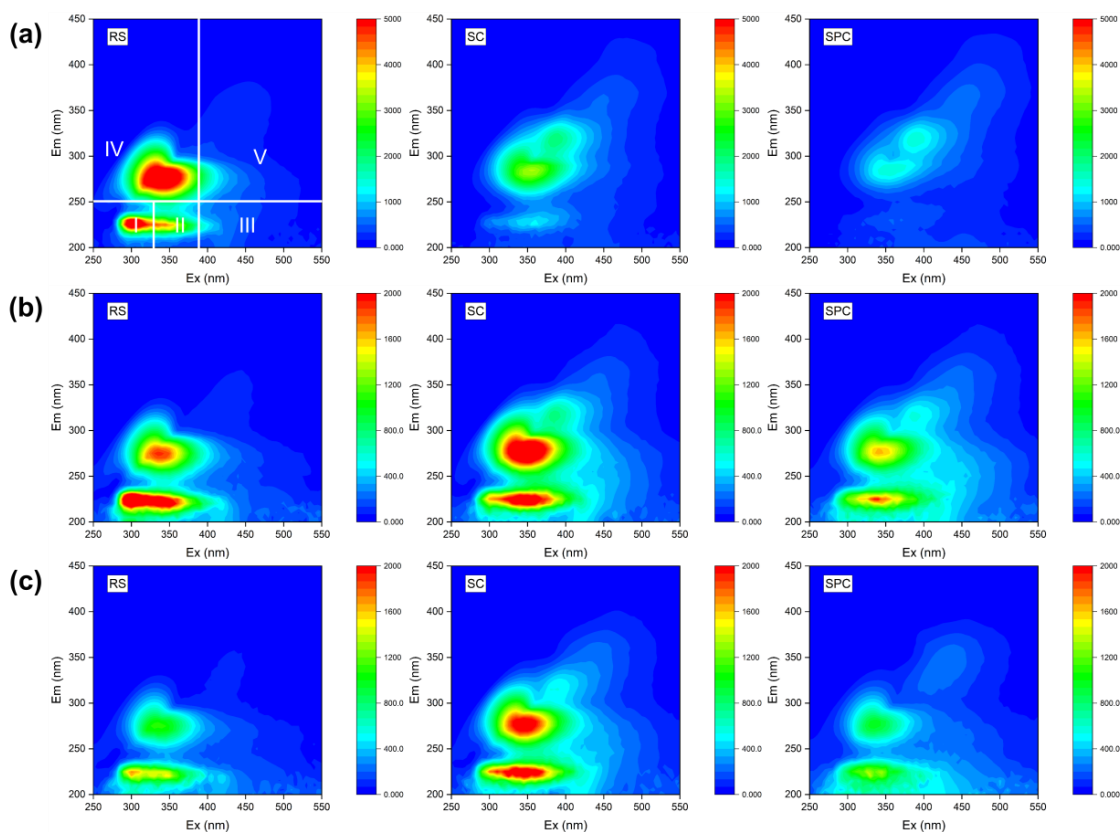


Figure 4. EEM spectra of EPS extracted from different sludge: (a) S-EPS, (b) LB-EPS, (c) TB-EPS. RS, heating treatment (80 °C, 35 min); SC, heating treatment (80 °C, 35 min) with SC; SPC, heating treatment (80 °C, 35 min) with SPC.

The fluorescence regional integration (FRI) of the EEM spectra was used for semi-quantitative analysis of the different EPS fractions (Table 2). The intensities of Region V in S-EPS were significantly increased compared to RS, while that of Region IV showed an opposite trend. In the TB-EPS, the intensity of Region IV was prominent, while it was less than half of that in RS and SPC. Overall, almost all the intensities of SPC were smaller than SC, implying the decomposition of EPS contents using SPC.

Table 2. Fluorescent intensities of EPS using different treatments.

EPS Fractions	Samples	I	II	III	IV	V
S-EPS	RS	19,076.33	14,560.01	10,746.11	48,497.00	17,251.53
	SC	3834.31	5955.42	8636.46	28,679.75	29,275.10
	SPC	2307.45	3159.86	7290.10	14,318.38	26,475.90
LB-EPS	RS	10,988.54	8012.61	6263.63	14,057.92	5123.95
	SC	7730.52	9694.10	10,094.36	21,187.43	14,179.75
	SPC	7020.12	7378.08	10,213.35	14,069.63	13,261.43
TB-EPS	RS	6836.05	5028.91	5298.01	8150.83	4064.37
	SC	7817.05	9008.21	9380.95	17,656.38	12,310.77
	SPC	6405.86	5434.81	7984.11	8160.08	8061.20

3.3. The Properties of ALE Products

3.3.1. Monosaccharides Composition of ALE

Monosaccharides are the basic building blocks of polysaccharides, and thus the components of monosaccharides can reflect the functional properties of polysaccharides. Figure 5 shows the monosaccharide composition of ALE extracted using the heating-SC and heating-SPC methods. The most common monosaccharides, including fucose (Fuc), arabinose (Ara), rhamnose (Rha), galactose (Gal), glucose (Glc), xylose (Xyl), mannose (Man), fructose (Fru), ribose (Rib), galacturonic acid (Gal-UA), glucuronic acid (Glc-UA), mannuronic acid (Man-UA), and guluronic acid (Gul-UA) in the ALE samples were identified and determined. The results clearly indicated that the two extracts had a very similar composition; the concentrations of monosaccharides were slightly reduced in the ALE using the heating-SPC method. Hence, it can be considered that the heating-SPC method hardly affects the structure and bioactivity of ALE from the perspective of monosaccharide composition. The total concentrations of monosaccharides were 81.00 and 74.60 mg/g in SC and SPC, respectively. The extracted ALEs in this study were hetero-polysaccharides, as they contained multiple (in this case, thirteen) types of monosaccharides. In total, 10 of the 13 types of monosaccharides were detected in both of the two ALE products, and only Fru, Gul-UA, and Man-UA were below the limit of detection. The molar percentages of these thirteen monosaccharides in the ALEs were determined and their proportions in the ALEs varied significantly. The two most prevalent monosaccharides were galactose (28.60–30.32%) and glucose (17.10–18.51%), and thus these are likely to form the carbon framework of the ALEs. Galactose was proven to relate to the anti-oxidant activity of polysaccharides and glucose was the most widely distributed monosaccharide [40]. In addition to the reported applications of the coating materials and biosorbents, this study also hints at the biological applications in the pharmaceutical industry.

3.3.2. Surface Functional Groups

To dig deeper into the atomic compositions of the ALEs, a full scan of the XPS spectrum in the binding energy range between 0 and 1200 eV was obtained. As demonstrated in Figure 6, the main peaks of C 1s (~286 eV) and O 1s (~532 eV) were identified in the full scan of the XPS spectra, denoting the high elemental proportions of C and O in the ALEs. The signal related to the Na element at the position of ~1072 eV mainly originated from the ALE extraction process, in which Na⁺ resided from SC or SPC.

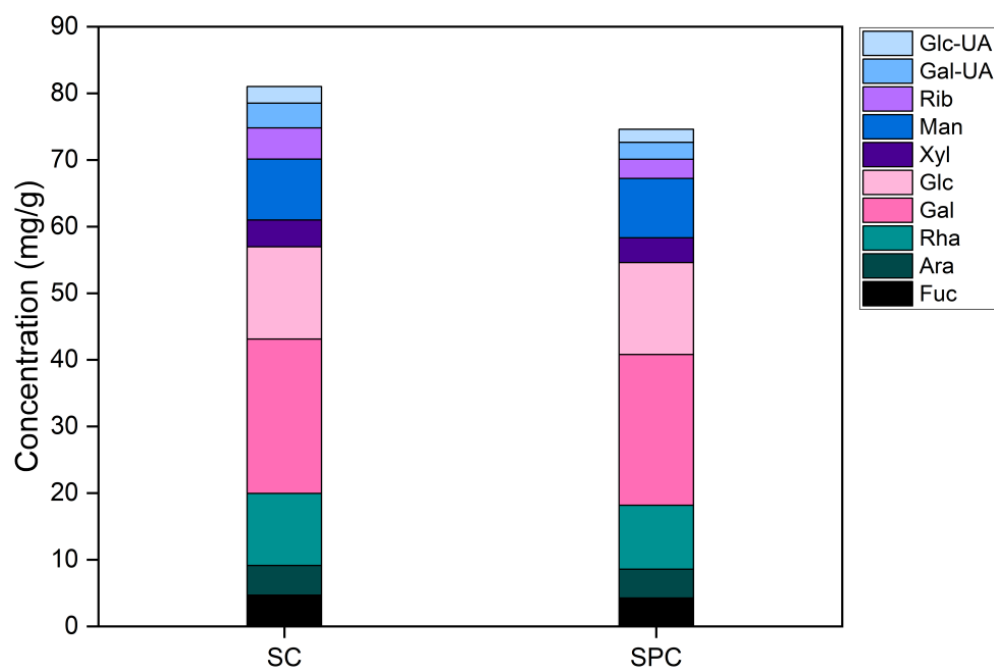


Figure 5. The monosaccharide composition of ALEs.

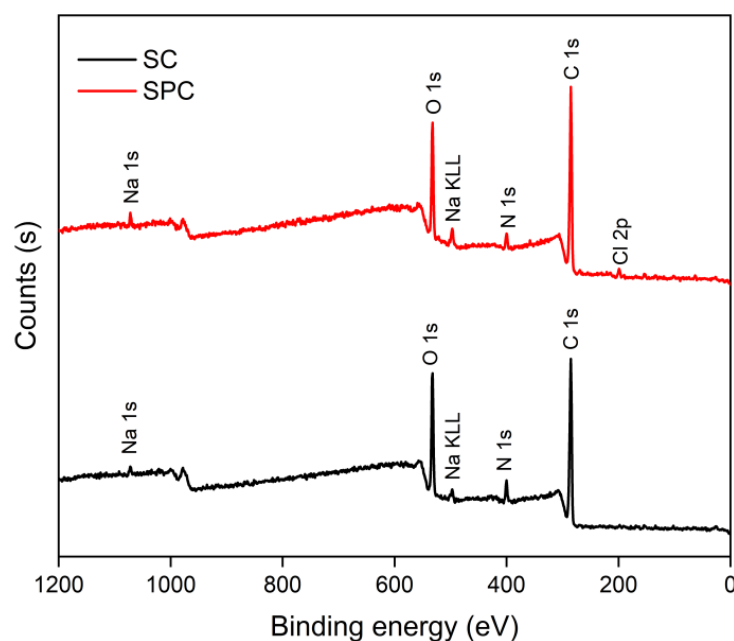


Figure 6. The full scan of X-ray photoelectron spectroscopy in ALEs.

Furthermore, the high-resolution spectrum of C 1s, N 1s, O 1s, and S 2p were collected and divided to obtain more detailed information on the chemical functionalities of ALEs (Figure 7). The C 1s XPS spectrum can be deconvoluted into four or three peaks. The peak at 284.8 eV belongs to C-(C/H), primarily from hydrocarbon-like molecules, including amino acids, polysaccharides, or lipids [41]. This was also the most prominent functional group in both the two ALEs with a proportion of ~65%. The peak at 286.3 eV was reported to be associated with the C-(O/N) from alcohol, amide, or ether amine groups (in proteins and polysaccharides) [41]. The peak at 287.01 eV corresponded to O=C-NH-, which was only present in the ALE extracted using SC. In addition, the peak at 287.8 eV related to C=O/O-C-O is usually involved in amide, carboxylate, acetal, or hemiacetal. The peak at 288.2 eV indicated the O=C-OH from carboxyl or ester moieties [42], which are only present

in SC. Compared with the ALE from SC, the types of functional groups of carbon were decreased in that of SPC, which may be due to the attack of free radicals induced by SPC.

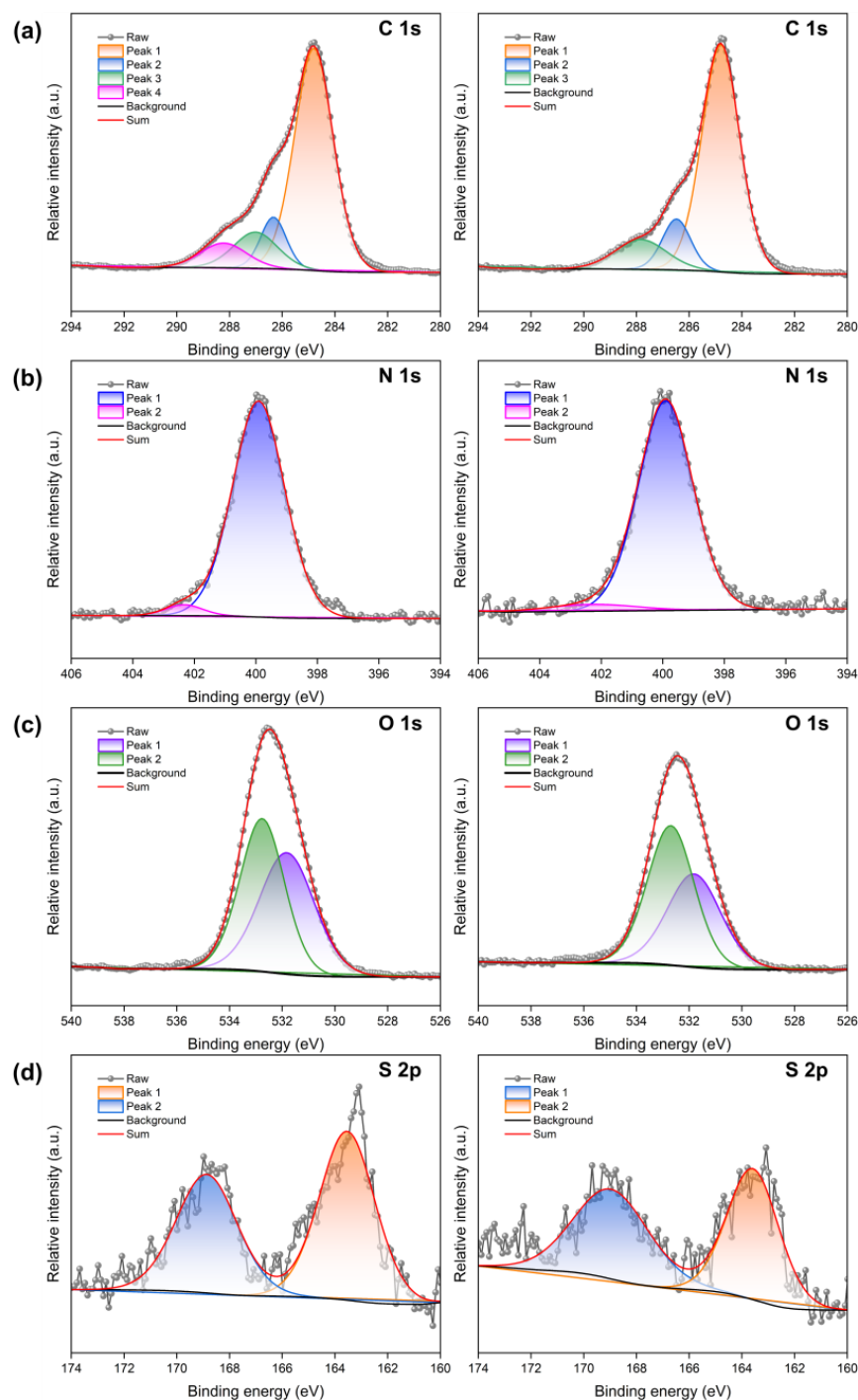


Figure 7. High-resolution scans: (a) C 1s, (b) O 1s, (c) N 1s, and (d) S 2p of X-ray photoelectron spectroscopy in ALEs. The left column represents SC; the right column represents SPC.

The N 1s peak can be resolved into two major peaks. The peak at 399.9 eV was attributed to the non-protonated nitrogen from the amines or amides, while the peak at 402.0 eV was assigned to the protonated amine from the amino acids or amino sugars [42]. The protonated amine increased from 3.46% (SC) to 5.04% (SPC) with a slight decrease in the non-protonated nitrogen.

The O 1s spectrum was also decomposed into two major peaks centered at ~531.0 eV (O=C), and ~532.2 eV (C-O-C, C-O-H). The percentage of O=C significantly decreased from 49.44% to 43.43%, which may be due to the oxidation induced by SPC. In conclusion, the surface functional groups of ALE altered.

The XPS spectra of S 2p were divided into two peaks at 163 eV and 169 eV, which were associated with the disulfide bonds (–S–S–) and –SO₃, respectively [43]. Disulfide bonds can influence the formation and stabilization of the conformational structure of proteins. The proportion of –S–S– considerably decreased from 56.53% (SC) to 49.97% (SPC), which may be due to SPC altering the protein conformations.

3.3.3. UV-Vis Spectrum of ALE

Figure 8a shows the UV-Vis spectra of the ALEs, together with the corresponding spectral parameter (S_R). Two primary absorbance bands in the region of 200–230 and 240–280 nm were resented in both the two ALEs. Previous studies have revealed that the band at 200–230 nm may be due to $n \rightarrow \pi^*$ electron transitions of the amide bond in the proteins, carboxyl, carbonyl, or ester. The other band (240–280 nm) may be related to $\pi \rightarrow \pi^*$ electron transitions in the aromatic and poly-aromatic organics, such as tryptophan and tyrosine in EPS [41]. It is evident that both the two ALEs contain similar functional groups related to proteins and polysaccharides, which were the most important active ingredients [14]. The significant absorption peaks near 260 nm usually indicate the presence of nucleic acids [44], thus it can be inferred that the extracted ALEs may contain nucleic acids. As a reference, no obvious absorption peak could be observed in the UV-Vis spectrum of the commercial sodium alginate, implying a relatively pure structure.

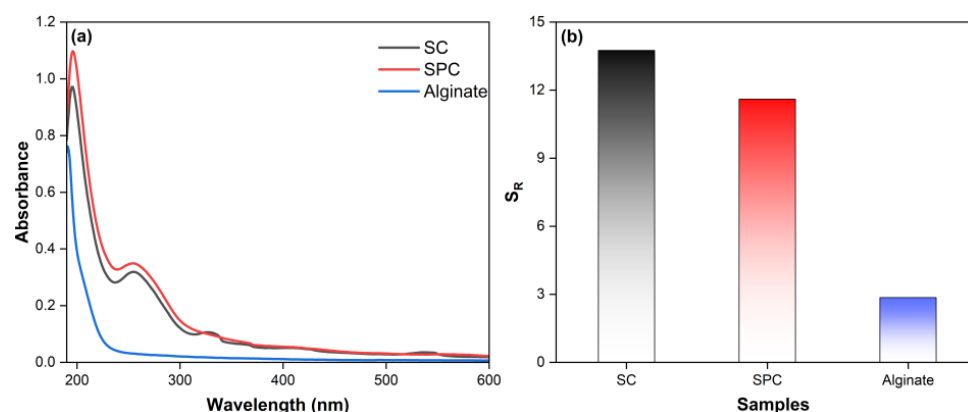


Figure 8. (a) UV-Vis spectra and (b) spectral slope parameters (S_R) of ALEs.

It is well known that the absorption region is mainly the result of electronic transition. The red shift of the UV-Vis spectrum usually implies a reduction in the energy required for electron transition, which also suggests the variation of molecular structures. It was reported that the absorption peak of unsaturated functional groups (such as conjugated and double bond systems) has a trend for red-shift, in which electrons are more easily affected by low-energy protons [41]. In this study, the red-shift phenomenon of the UV-Vis spectrum in ALE using SPC compared to SC may be due to the newly formed unsaturated compounds. In addition, the peak at 330 nm in SC results from the $n \rightarrow \pi^*$ electronic transition of the quinolones nitrogen atom in ciprofloxacin [45]; however, it disappeared in SPC, indicating the decomposition of the quinolones group using SPC. Figure 8b demonstrated that the S_R of SPC was smaller than that of SC, indicating an increase in molecular weight [46]. In addition, both the S_R values of SC and SPC are lower than that of commercial alginate, denoting a lower molecular weight.

3.3.4. ^1H NMR Spectra of ALEs

The ^1H NMR spectra of the dissolved organic fraction of sludge also confirms the difference of functional groups in SC and SPC (Figure 9). According to their different distribution areas, the spectra can be roughly divided into three categories: (1) H_{Ali} (0–3 ppm), characterizing terminal methyl groups of methylene chains, protons on methyl groups of highly branched aliphatic structure, and protons on aliphatic carbons which are two or more carbons away from the aromatic rings or polar functional groups; (2) $\text{H}_{\text{R-O}}$ (3–6.5 ppm), representing protons on carbons attached to O or N heteroatoms; and (3) H_{Ar} (6.5–10 ppm), signifying unhindered and sterically hindered aromatic protons [47].

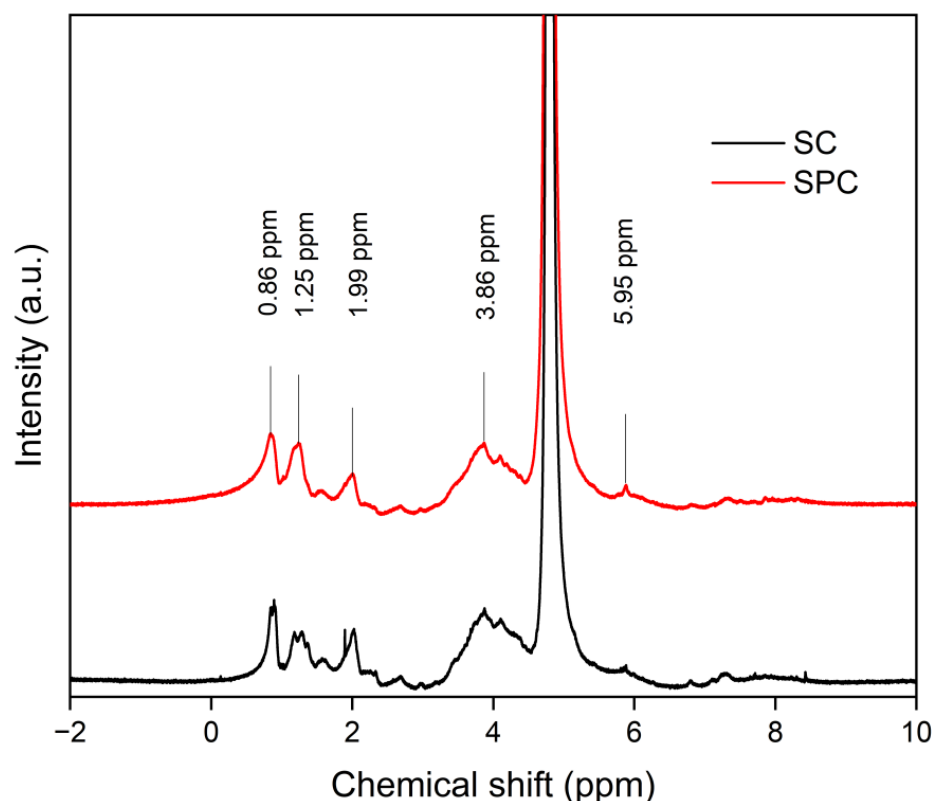


Figure 9. ^1H NMR spectra of ALEs.

In the H_{Ali} area, the following signals were observed: $\delta = 0.8, 1.3, 1.5, 1.9, 2.0,$ and 2.7 ppm. The peak centered at 0.8 ppm is related to the aliphatic CH_3 groups. The multiplet signal, with a maximum at 1.3 ppm, is mainly attributed to the aliphatic $-\text{CH}_2-$, although CH_3- bound to $-\text{C}-\text{O}-\text{R}$ groups ($\text{R} = \text{H}, \text{alkyl}, \text{Ph}, \text{COR}, \text{COPh}$) or $-\text{CH}_2-\beta$ to amine groups. It can be seen that the multiplet signal (0.8 ppm) in SC turned to a singlet one in SPC. The sharp singlet at $\delta = 1.9$ ppm is assigned to $-\text{CH}_2-\text{C}=\text{C}$, which was only present in SC while it disappeared in SPC. The signal at 2.0 ppm is probably attributed to $-\text{CH}_2-$ and CH_3- groups linked to $-\text{CONR}_2$, $-\text{COOR}$ or COR groups or to the CH_3-Ph group. The signal at $\delta = 2.7$ ppm originated from the aliphatic protons, which attached the C atom α to the benzene ring ($\text{Ph}-\text{C}_\alpha\text{H}_2-\text{C}_\beta\text{H}_2-\text{C}_\gamma\text{H}_2$) [48].

In the $\text{H}_{\text{R-O}}$ area, the broad band from 3.1 to 4.5 ppm and signal at 5.8 ppm were observed. Signals in this area originated from the $\text{CH}_3-\text{O}-$ and $-\text{CH}_2-\text{O}-$ groups. The signals in this area indicate a large variety of O-substituted compounds, or protons in the hydroxide groups of alcohols and phenols. The peaks between 3.2 and 4 ppm are also reported to associate with the pyranose ring [49].

In the H_{Ar} area, weak signals are observed: $\delta = 6.8, 7.3$ ppm and a sharp singlet at 8.4 ppm. The sharp singlet at 8.4 ppm can be assigned to the resonance of phenolic- OH

protons, which only presented in SC. The other peaks in the H_{Ar} region originate from the aromatic H and pyrrolic or indolic H, which were negligible in both SC and SPC.

3.4. Environmental Implications

Sludge treatment and resource recovery has been a long-standing problem in wastewater treatment plants. Extracellular biopolymers extracted from sludge were validated as a sustainable alternative for some existing chemical materials, such as flame-retardant composites and seed coating agents. However, the current research on biopolymer extraction mainly focuses on AGS, due to the relatively high content of EPS. The biopolymer yield from CAS was at a low level (9–9%), thus there is an urgent need for a more efficient method of ALE extraction. In this study, a simple alternative method to the conventional heating-SC protocol was proposed and demonstrated higher extraction efficiency for ALE extraction. This research could promote practical applications of resource recovery from waste-activated sludge while reducing the environmental burden.

4. Conclusions

ALE extraction from conventional waste-activated sludge could be improved by using SPC as a substitute for SC in the heating-SC protocol, and the alginate purity of the products could be also improved. The physical and chemical properties of sludge showed that SPC can effectively destroy sludge flocs and thus release the organic substances in it. In addition, the molecular structure of the extracted ALE may be changed due to the oxidizing properties of SPC. The molecular weight of ALE in SPC is larger than that in SC. The EEM spectra indicated the decomposition of organics in EPS, which was further confirmed by the 1H NMR spectra. This study proposes a new method of ALE extraction from conventional activated sludge. Future research is needed to optimize the technical parameters and perform techno-economic analysis. Based on this study, this new method has already shown great potential to turn waste into treasure and realize a circular economy.

Author Contributions: Conceptualization, X.L.; methodology, X.L. and F.L.; software, X.L.; validation, X.L.; formal analysis, X.L.; investigation, X.L. and W.R.; resources, Y.Z.; data curation, X.L. and Y.X.; writing—original draft preparation, X.L.; writing—review and editing, X.L.; visualization, X.L.; supervision, Y.Z. and Z.X.; project administration, Y.Z.; funding acquisition, Y.Z. All authors have read and agreed to the published version of the manuscript.

Funding: This research was funded by the National Natural Science Foundation of China, grant number 51679083.

Institutional Review Board Statement: Not applicable.

Informed Consent Statement: Not applicable.

Data Availability Statement: Not applicable.

Acknowledgments: All the sludge samples were obtained from the Kaifu District Wastewater Treatment Plant (Changsha, China), and special thanks are given to them for providing the experimental materials.

Conflicts of Interest: The authors declare no conflict of interest.

References

1. Liu, X.; Zhai, Y.; Xu, Z.; Liu, L.; Ren, W.; Xie, Y.; Li, C.; Zhu, Y.; Xu, M. Unraveling the Impacts of Cu^{3+} -Based Treatments on Sludge Dewaterability: The Overlooked Role of Cu^{3+} . *Chem. Eng. J.* **2023**, *457*, 141106. [[CrossRef](#)]
2. Siddiqui, M.I.; Rameez, H.; Farooqi, I.H.; Basheer, F. Recent Advancement in Commercial and Other Sustainable Techniques for Energy and Material Recovery from Sewage Sludge. *Water* **2023**, *15*, 948. [[CrossRef](#)]
3. Yu, H.-Q. Molecular Insights into Extracellular Polymeric Substances in Activated Sludge. *Environ. Sci. Technol.* **2020**, *54*, 7742–7750. [[CrossRef](#)]

4. Cao, B.; Zhang, T.; Zhang, W.; Wang, D. Enhanced Technology Based for Sewage Sludge Deep Dewatering: A Critical Review. *Water Res.* **2021**, *189*, 116650. [\[CrossRef\]](#)
5. Zhang, W.; Tang, M.; Li, D.; Yang, P.; Xu, S.; Wang, D. Effects of Alkalinity on Interaction between EPS and Hydroxy-Aluminum with Different Speciation in Wastewater Sludge Conditioning with Aluminum Based Inorganic Polymer Flocculant. *J. Environ. Sci.* **2021**, *100*, 257–268. [\[CrossRef\]](#)
6. Bahgat, N.T.; Wilfert, P.; Korving, L.; van Loosdrecht, M. Integrated Resource Recovery from Aerobic Granular Sludge Plants. *Water Res.* **2023**, *234*, 119819. [\[CrossRef\]](#) [\[PubMed\]](#)
7. Kim, N.K.; Mao, N.; Lin, R.; Bhattacharyya, D.; van Loosdrecht, M.C.M.; Lin, Y. Flame Retardant Property of Flax Fabrics Coated by Extracellular Polymeric Substances Recovered from Both Activated Sludge and Aerobic Granular Sludge. *Water Res.* **2020**, *170*, 115344. [\[CrossRef\]](#) [\[PubMed\]](#)
8. Chen, X.; Lee, Y.-J.; Yuan, T.; Lei, Z.; Adachi, Y.; Zhang, Z.; Lin, Y.; van Loosdrecht, M.C.M. A Review on Recovery of Extracellular Biopolymers from Flocculent and Granular Activated Sludges: Cognition, Key Influencing Factors, Applications, and Challenges. *Bioresour. Technol.* **2022**, *363*, 127854. [\[CrossRef\]](#)
9. Sheng, G.-P.; Yu, H.-Q.; Li, X.-Y. Extracellular Polymeric Substances (EPS) of Microbial Aggregates in Biological Wastewater Treatment Systems: A Review. *Biotechnol. Adv.* **2010**, *28*, 882–894. [\[CrossRef\]](#)
10. Lin, Y.M.; Sharma, P.K.; van Loosdrecht, M.C.M. The Chemical and Mechanical Differences between Alginate-like Exopolysaccharides Isolated from Aerobic Flocculent Sludge and Aerobic Granular Sludge. *Water Res.* **2013**, *47*, 57–65. [\[CrossRef\]](#)
11. Lin, Y.; de Kreuk, M.; van Loosdrecht, M.C.M.; Adin, A. Characterization of Alginate-like Exopolysaccharides Isolated from Aerobic Granular Sludge in Pilot-Plant. *Water Res.* **2010**, *44*, 3355–3364. [\[CrossRef\]](#) [\[PubMed\]](#)
12. Lin, Y.M.; Nierop, K.G.J.; Girbal-Neuhauser, E.; Adriaanse, M.; van Loosdrecht, M.C.M. Sustainable Polysaccharide-Based Biomaterial Recovered from Waste Aerobic Granular Sludge as a Surface Coating Material. *Sustain. Mater. Technol.* **2015**, *4*, 24–29. [\[CrossRef\]](#)
13. de Amorim de Carvalho, C.; Ferreira dos Santos, A.; Tavares Ferreira, T.J.; Sousa Aguiar Lira, V.N.; Mendes Barros, A.R.; Bezerra dos Santos, A. Resource Recovery in Aerobic Granular Sludge Systems: Is It Feasible or Still a Long Way to Go? *Chemosphere* **2021**, *274*, 129881. [\[CrossRef\]](#)
14. Li, J.; Hao, X.; Gan, W.; van Loosdrecht, M.C.M.; Wu, Y. Enhancing Extraction of Alginate like Extracellular Polymers (ALE) from Flocculent Sludge by Surfactants. *Sci. Total Environ.* **2022**, *837*, 155673. [\[CrossRef\]](#) [\[PubMed\]](#)
15. Lin, Y.M.; Wang, L.; Chi, Z.M.; Liu, X.Y. Bacterial Alginate Role in Aerobic Granular Bio-particles Formation and Settability Improvement. *Sep. Sci. Technol.* **2008**, *43*, 1642–1652. [\[CrossRef\]](#)
16. Feng, C.; Lotti, T.; Lin, Y.; Malpei, F. Extracellular Polymeric Substances Extraction and Recovery from Anammox Granules: Evaluation of Methods and Protocol Development. *Chem. Eng. J.* **2019**, *374*, 112–122. [\[CrossRef\]](#)
17. Li, Y.; Zhu, Y.; Wang, D.; Yang, G.; Pan, L.; Wang, Q.; Ni, B.-J.; Li, H.; Yuan, X.; Jiang, L.; et al. Fe(II) Catalyzing Sodium Percarbonate Facilitates the Dewaterability of Waste Activated Sludge: Performance, Mechanism, and Implication. *Water Res.* **2020**, *174*, 115626. [\[CrossRef\]](#)
18. Mo, Z.; Tan, Z.; Liang, J.; Guan, Z.; Liao, X.; Jian, J.; Liu, H.; Li, Y.; Dai, W.; Sun, S. Iron-Rich Sludge Biochar Triggers Sodium Percarbonate Activation for Robust Sulfamethoxazole Removal: Collaborative Roles of Reactive Oxygen Species and Electron Transfer. *Chem. Eng. J.* **2023**, *457*, 141150. [\[CrossRef\]](#)
19. Liang, J.; Tan, Z.; Zhang, L.; Li, C.; Mo, Z.; Ye, M.; Ai, J.; Huang, S.; Sun, S.; Liu, H. Chalcopyrite-Activated Sodium Percarbonate Oxidation for Sludge Dewaterability Enhancement: Synergetic Roles of $\bullet\text{OH}$ and $^1\text{O}_2$. *Chem. Eng. J.* **2023**, *465*, 142863. [\[CrossRef\]](#)
20. Wang, Y.; Wang, X.; Zheng, K.; Guo, H.; Tian, L.; Zhu, T.; Liu, Y. Ultrasound-Sodium Percarbonate Effectively Promotes Short-Chain Carboxylic Acids Production from Sewage Sludge through Anaerobic Fermentation. *Bioresour. Technol.* **2022**, *364*, 128024. [\[CrossRef\]](#)
21. Wang, Y.; Sun, P.; Guo, H.; Zheng, K.; Zhu, T.; Liu, Y. Performance and Mechanism of Sodium Percarbonate (SPC) Enhancing Short-Chain Fatty Acids Production from Anaerobic Waste Activated Sludge Fermentation. *J. Environ. Manag.* **2022**, *313*, 115025. [\[CrossRef\]](#)
22. Zhang, Q.; Cheng, X.; Wang, F.; Fang, S.; Zhang, L.; Huang, W.; Fang, F.; Cao, J.; Luo, J. Unveiling the Behaviors and Mechanisms of Percarbonate on the Sludge Anaerobic Fermentation for Volatile Fatty Acids Production. *Sci. Total Environ.* **2022**, *838*, 156054. [\[CrossRef\]](#) [\[PubMed\]](#)
23. Wang, Y.; Zheng, K.; Ding, J.; Guo, H.; Chen, X.; Zhu, T.; Sun, P.; Liu, Y. Ultrasonic Radiation Enhances Percarbonate Oxidation for Improving Anaerobic Digestion of Waste Activated Sludge. *Chem. Eng. J.* **2023**, *457*, 141178. [\[CrossRef\]](#)
24. Wang, Y.; Sun, P.; Guo, H.; Wang, D.; Zhu, T.; Liu, Y. Enhancing Methane Production from Anaerobic Digestion of Waste Activated Sludge through a Novel Sodium Percarbonate (SPC) Pretreatment: Reaction Kinetics and Mechanisms. *ACS ES&T Eng.* **2022**, *2*, 1326–1340. [\[CrossRef\]](#)
25. Ling, X.; Deng, J.; Ye, C.; Cai, A.; Ruan, S.; Chen, M.; Li, X. Fe(II)-Activated Sodium Percarbonate for Improving Sludge Dewaterability: Experimental and Theoretical Investigation Combined with the Evaluation of Subsequent Utilization. *Sci. Total Environ.* **2021**, *799*, 149382. [\[CrossRef\]](#) [\[PubMed\]](#)

26. Li, Y.; Wang, D.; Yang, G.; Yuan, X.; Yuan, L.; Li, Z.; Xu, Q.; Liu, X.; Yang, Q.; Tang, W.; et al. In-Depth Research on Percarbonate Expediting Zero-Valent Iron Corrosion for Conditioning Anaerobically Digested Sludge. *J. Hazard. Mater.* **2021**, *419*, 126389. [\[CrossRef\]](#)
27. Yue, L.; Cheng, J.; Hua, J.; Dong, H.; Zhou, J. A Sodium Percarbonate/Ultraviolet System Generated Free Radicals for Degrading Capsaicin to Alleviate Inhibition of Methane Production during Anaerobic Digestion of Lipids and Food Waste. *Sci. Total Environ.* **2021**, *761*, 143269. [\[CrossRef\]](#)
28. Li, J.; Hao, X.; Gan, W.; van Loosdrecht, M.C.M.; Wu, Y. Controlling Factors and Involved Mechanisms on Forming Alginate like Extracellular Polymers in Flocculent Sludge. *Chem. Eng. J.* **2022**, *439*, 135792. [\[CrossRef\]](#)
29. Li, J.; Hao, X.; Gan, W.; van Loosdrecht, M.C.M.; Wu, Y. Recovery of Extracellular Biopolymers from Conventional Activated Sludge: Potential, Characteristics and Limitation. *Water Res.* **2021**, *205*, 117706. [\[CrossRef\]](#)
30. APHA. *Standard Methods For the Examination of Water and Wastewater*; American Public Health Association: Washington, DC, USA, 2009.
31. Liu, X.; Zhai, Y.; Xu, Z.; Zhu, Y.; Zhou, Y.; Wang, Z.; Liu, L.; Liang, F.; Ren, W.; Xie, Y.; et al. One-Pot Production of 5-Methylfurfural (5-MF) and Enhanced Dewaterability of Waste Activated Sludge by Hydrothermal Treatment with Natural Deep Eutectic Solvents (NADES): Experimental and Theoretical Studies. *Chem. Eng. J.* **2023**, *464*, 142575. [\[CrossRef\]](#)
32. Zhen, G.; Lu, X.; Zhao, Y.; Chai, X.; Niu, D. Enhanced Dewaterability of Sewage Sludge in the Presence of Fe(II)-Activated Persulfate Oxidation. *Bioresour. Technol.* **2012**, *116*, 259–265. [\[CrossRef\]](#)
33. Guo, L.; Lu, M.; Li, Q.; Zhang, J.; Zong, Y.; She, Z. Three-Dimensional Fluorescence Excitation–Emission Matrix (EEM) Spectroscopy with Regional Integration Analysis for Assessing Waste Sludge Hydrolysis Treated with Multi-Enzyme and Thermophilic Bacteria. *Bioresour. Technol.* **2014**, *171*, 22–28. [\[CrossRef\]](#)
34. Helms, J.R.; Stubbins, A.; Ritchie, J.D.; Minor, E.C.; Kieber, D.J.; Mopper, K. Absorption Spectral Slopes and Slope Ratios as Indicators of Molecular Weight, Source, and Photobleaching of Chromophoric Dissolved Organic Matter. *Limnol. Oceanogr.* **2008**, *53*, 955–969. [\[CrossRef\]](#)
35. Xing, Y.; Huang, X.; Wang, H.; Yu, J. Insight in the Mechanism of Alkali Treatment Methods Effecting Dewatered Sludge Fermentation from Microbial Characteristics. *J. Environ. Chem. Eng.* **2022**, *10*, 108861. [\[CrossRef\]](#)
36. Chen, W.; Westerhoff, P.; Leenheer, J.A.; Booksh, K. Fluorescence Excitation–Emission Matrix Regional Integration to Quantify Spectra for Dissolved Organic Matter. *Environ. Sci. Technol.* **2003**, *37*, 5701–5710. [\[CrossRef\]](#) [\[PubMed\]](#)
37. Liu, R.; Yu, X.; Yu, P.; Guo, X.; Zhang, B.; Xiao, B. New Insights into the Effect of Thermal Treatment on Sludge Dewaterability. *Sci. Total Environ.* **2019**, *656*, 1082–1090. [\[CrossRef\]](#) [\[PubMed\]](#)
38. Gonzalez, A.; van Lier, J.B.; de Kreuk, M.K. Effects of Mild Thermal Pre-Treatment Combined with H₂O₂ Addition on Waste Activated Sludge Digestibility. *Waste Manag.* **2022**, *141*, 163–172. [\[CrossRef\]](#) [\[PubMed\]](#)
39. Aftab, B.; Truong, H.B.; Cho, J.; Hur, J. Enhanced Performance of a Direct Contact Membrane Distillation System via In-Situ Thermally Activated H₂O₂ Oxidation for the Treatment of Landfill Leachate. *J. Membr. Sci.* **2022**, *652*, 120478. [\[CrossRef\]](#)
40. Liu, J.; Zhang, Z.; Deng, Y.; Sato, Y.; Wu, D.; Chen, G. Coupling Methane and Bioactive Polysaccharide Recovery from Wasted Activated Sludge: A Sustainable Strategy for Sludge Treatment. *Water Res.* **2023**, *233*, 119775. [\[CrossRef\]](#) [\[PubMed\]](#)
41. Wang, B.-B.; Liu, X.-T.; Chen, J.-M.; Peng, D.-C.; He, F. Composition and Functional Group Characterization of Extracellular Polymeric Substances (EPS) in Activated Sludge: The Impacts of Polymerization Degree of Proteinaceous Substrates. *Water Res.* **2018**, *129*, 133–142. [\[CrossRef\]](#)
42. Wu, C.; Chen, Y.; Qian, Z.; Chen, H.; Li, W.; Li, Q.; Xue, S. The Effect of Extracellular Polymeric Substances (EPS) of Iron-Oxidizing Bacteria (*Ochrobactrum* EEELCW01) on Mineral Transformation and Arsenic (As) Fate. *J. Environ. Sci.* **2023**, *130*, 187–196. [\[CrossRef\]](#)
43. Sha, L.; Wu, Z.; Ling, Z.; Liu, X.; Yu, X.; Zhang, S. Investigation on the Improvement of Activated Sludge Dewaterability Using Different Iron Forms (ZVI vs. Fe(II))/Peroxydisulfate Combined Vertical Electro-Dewatering Processes. *Chemosphere* **2022**, *292*, 133416. [\[CrossRef\]](#) [\[PubMed\]](#)
44. Liu, M.; Meng, P.; Chen, G.; Guan, Y.; Liu, G. Correlation of Structural Extracellular Polymeric Substances in the Mesh Biofilms with Solids Retention Time and Biofilm Hydraulic Resistance in Dynamic Membrane Bioreactors. *Sci. Total Environ.* **2022**, *832*, 155000. [\[CrossRef\]](#) [\[PubMed\]](#)
45. Lu, C.; Gu, J.; Wei, G.; Ba, J.; Zhang, L.; Li, Z.; Pei, R.; Li, J.; Wei, J. Three-Dimensional Electro-Fenton Degradation of Ciprofloxacin Catalyzed by CuO Doped Red Mud Particle Electrodes: Influencing Factors, Possible Degradation Pathways and Energy Consumption. *J. Environ. Chem. Eng.* **2022**, *10*, 107737. [\[CrossRef\]](#)
46. Yin, C.; Meng, F.; Meng, Y.; Chen, G.-H. Differential Ultraviolet–Visible Absorbance Spectra for Characterizing Metal Ions Binding onto Extracellular Polymeric Substances in Different Mixed Microbial Cultures. *Chemosphere* **2016**, *159*, 267–274. [\[CrossRef\]](#)
47. Wang, Q.; Xu, Q.; Du, Z.; Zhang, W.; Wang, D.; Peng, Y. Mechanistic Insights into the Effects of Biopolymer Conversion on Macroscopic Physical Properties of Waste Activated Sludge during Hydrothermal Treatment: Importance of the Maillard Reaction. *Sci. Total Environ.* **2021**, *769*, 144798. [\[CrossRef\]](#)

48. Bartoszek, M.; Polak, J.; Sułkowski, W.W. NMR Study of the Humification Process during Sewage Sludge Treatment. *Chemosphere* **2008**, *73*, 1465–1470. [[CrossRef](#)]
49. Pronk, M.; Neu, T.R.; van Loosdrecht, M.C.M.; Lin, Y.M. The Acid Soluble Extracellular Polymeric Substance of Aerobic Granular Sludge Dominated by *Deftluviicoccus* sp. *Water Res.* **2017**, *122*, 148–158. [[CrossRef](#)]

Disclaimer/Publisher’s Note: The statements, opinions and data contained in all publications are solely those of the individual author(s) and contributor(s) and not of MDPI and/or the editor(s). MDPI and/or the editor(s) disclaim responsibility for any injury to people or property resulting from any ideas, methods, instructions or products referred to in the content.